Available online at www.sciencedirect.com

ScienceDirect

Ceramics International 38 (2012) 449–456

CERAMICS INTERNATIONAL

www.elsevier.com/locate/ceramint

A simple and efficient preparation of $LaFeO_3$ nanopowders by glycine–nitrate process: Effect of glycine concentration

Rajender R. Kondakindi *, Kunal Karan, Brant A. Peppley **

Queen's-RMC Fuel Cell Research Centre, 945 Princess St., Kingston, Ontario, Canada K7L 5L9

Received 28 May 2011; received in revised form 13 July 2011; accepted 14 July 2011

Abstract

$LaFeO_3$ perovskites have been prepared by the glycine–nitrate process (GNP) at various glycine-to-nitrate molar ratios. The perovskites have been systematically characterized by X-ray diffraction, BET surface area, scanning electron microscopy, transmission electron microscopy and temperature-programmed reduction to study the effect of glycine concentration on various properties of $LaFeO_3$. The X-ray diffraction patterns of the as-prepared and calcined samples show the formation of orthorhombic phase without any impurities. The BET specific surface areas of various perovskites increased with an increase in glycine-to-nitrate ratio (GNR) of 2.0 but were nearly constant at higher ratios. The scanning electron microscopy indicates that the prepared material is flake-like at GNRs $\leq$1.5 and exists as agglomerated particles at GNRs $\geq$2.0. The particle size of the as-prepared samples was in the range of 30–130 nm depending on the GNR and the calcined samples exhibited particle size in the range of 60–160 nm. The samples that were prepared at GNR $<$ 1.5 did not show any peaks in temperature-programmed reduction, but the samples prepared at a GNR of 2.0 and above showed the reduction of Fe^{n+}.

Keywords: $LaFeO_3$; Combustion; X-ray diffraction; Surface area; Particle size; Reducibility

1. Introduction

Perovskites are ABO_3 type structured materials with a rare earth metal at the A-site and a transition metal at the B-site. The ionic radius of the A-ion is larger than 1.0 Å, while the size of the B-ion is in the order of 0.6–0.8 Å. Perovskites have been considered for various applications including catalysis [1–3], solid oxide fuel cells [4–7], gas sensors [8] and as magnetic materials [9,10]. One of the common perovskites is $LaFeO_3$, which has been reported for studies on Fischer–Tropsch synthesis [11], partial oxidation of methane [12,13] and diesel reformation [14]. Methods for preparation of $LaFeO_3$ perovskite include solid-state method [15], coprecipitation [16], sol–gel method [17], citrate-gel method [18] and combustion method [16,19]. These synthesis methods result in materials that differ in microstructure, porosity and surface area. In the conventional solid state method, the oxides/carbonates are ground and fired at high temperatures (~1000 °C). This method leads to large particle size and might result in secondary phases as impurities due to high temperature treatment. The wet chemical methods result in fine particles that are homogeneous in size but require long preparation time and calcination at a specific temperature depending on the final requirements for the catalyst. In recent years, combustion method has attracted significant interest due to its simplicity [16,19]. Although synthesis of $LaFeO_3$ by combustion method has been reported [16,19], there is a lack of information on the influence of glycine concentration on various properties of $LaFeO_3$.

In the present study, $LaFeO_3$ perovskites have been prepared by the glycine–nitrate process (GNP) with different amounts of glycine and at different preparation temperatures to investigate the effect of these parameters on surface area, particle size, microstructure and reducibility. The synthesized perovskites were characterized by X-ray diffraction to confirm the phase purity, by BET for surface area, by transmission electron microscopy for particle size and by temperature-programmed reduction to study the reducibility. The results obtained from the characterization are discussed in the light of preparation conditions.

---

* Corresponding author. Present address: College of Science, Technology, Engineering and Mathematics, Youngstown State University, One university Plaza, Youngstown, OH 44555, USA.

** Corresponding author. Tel.: +1 613 533 3247.

E-mail address: rajender.kondakindi@gmail.com (R.R. Kondakindi).

0272-8842/$36.00 © 2011 Elsevier Ltd and Techna Group S.r.l. All rights reserved.
doi:10.1016/j.ceramint.2011.07.026

2. Experimental

2.1. Preparation of perovskites

$LaFeO_3$ perovskites have been prepared by the combustion method using glycine as the fuel. Lanthanum nitrate ($La(NO_3)_3 \cdot 6H_2O$, 99.9%), iron nitrate ($Fe(NO_3)_3 \cdot 9H_2O$, 99.98%) and glycine (NH_2CH_2COOH, 99.5%) were obtained from Alfa Aesar, USA. Glycine-to-nitrate ratio (GNR) has been calculated based on the oxidizing and the reducing valencies of nitrate and glycine, respectively. The oxidizing valency of lanthanum nitrate is −15 ($La(NO_3)_3 = 3 + 3(0 + (-6)) = -15$) and the reducing valency of glycine is +9 ($H_2NCH_2COOH = 2(1) + 0 + 4 + 2 + 4 - 2 - 2 + 1 = +9$). Hence, 1 mol of lanthanum nitrate requires 1.66 mol of glycine (GNR = 1.0). In a typical GNP, nitrates of lanthanum and iron were dissolved in 50 ml of deionized water in a beaker (2 g batch). Glycine was added to this nitrate solution according to the desired GNR. The solution, while being stirred, was heated on a hot plate to vaporize most of the water. Once the solution became sufficiently thick to initiate combustion, the beaker was placed in a furnace maintained at 300 °C. $LaFeO_3$ samples were synthesized at a furnace temperature of 300 °C with 8 different GNRs ranging from 0.75 to 4.0. Additional two samples were prepared at 100 °C and at 450 °C at a GNR of 2.0 to study the effect of preparation temperature on the morphology and BET specific surface area. All the powders obtained after the combustion were ground, sieved through no. 100 mesh and finally calcined at 700 °C for 2 h.

2.2. Characterization

X-ray diffraction patterns were recorded on a Scintag X-ray diffractometer with Cu Kα radiation in the 2θ range 20–80°. The particle size has been calculated by Scherrer equation after subtracting the instrument broadening. The BET specific surface areas were measured on an Autosorb-I instrument at liquid nitrogen temperature. The samples were degassed at 200 °C for 2 h before the analysis. Mossbauer spectroscopy in transmission and constant acceleration mode was performed with a ^{57}Co in Rh matrix. The isomer shifts are reported with respect to α-Fe. The analysis was carried out at room temperature. Scanning electron micrographs of perovskite samples were recorded on a Philips XL30 instrument after gold coating the samples. The samples for transmission electron microscopy analysis were prepared by dispersing sample powders in ethanol followed by spraying onto Cu grids using an air gun. Transmission electron micrographs of various samples were recorded on a Philips CM20 instrument at 200 kV.

Temperature-programmed reduction experiments were carried out on a Zeton Altamira AMI-200 instrument. Approximately, 0.03 g of the catalyst was loaded in a quartz tube and held between two quartz wool plugs. The temperature of the catalyst was measured using a thermocouple that was in contact with the sample. The sample was pretreated at 300 °C for 30 min in a flow of Ar (50 ml/min). After the pretreatment, the reactor was cooled to room temperature and the gas flow changed to 10 vol.% H_2 in H_2/Ar mixture (50 ml/min). The sample temperature was then ramped to 900 °C at a heating rate of 10 °C/min. The change in the thermal conductivity of the gas mixture, due to hydrogen consumption, was measured as the signal.

3. Results and discussion

3.1. X-ray diffraction (XRD)

XRD patterns of the as-prepared $LaFeO_3$ perovskites are shown in Fig. 1. All the prepared samples are in the orthorhombic phase without any impurities such as single oxides/metal. The phase formation was also confirmed after the calcination step at 700 °C (Fig. 2). It is important to note that the intensities are not normalized in Figs. 1 and 2 and, hence,

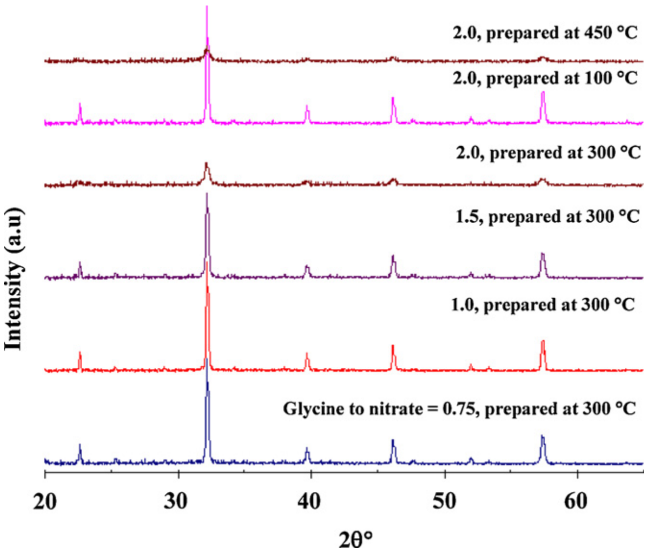

Fig. 1. X-ray diffraction patterns of the as-prepared $LaFeO_3$ perovskites.

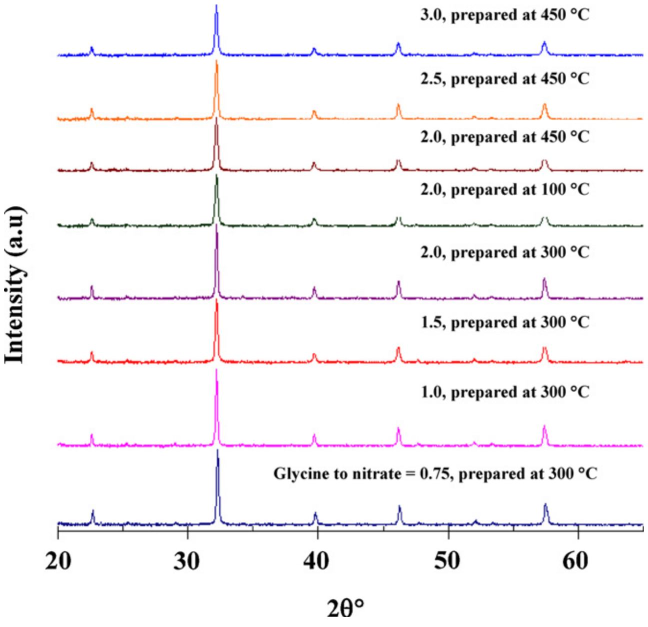

Fig. 2. X-ray diffraction patterns of the calcined perovskites.

Table 1
BET areas and particle sizes of various $LaFeO_3$ perovskites.

S.no.	Glycine to nitrate molar ratio	BET area (m^2/g)[c]	Particle size (nm)	
			BET[c]	XRD[c]
1	0.75	7.8/6.9	116/131	109/115
2	1.0	6.5/5.7	139/158	134/139
3	1.5	14.3/10.5	63/86	75/85
4	2.0	26.2/13.5	34/67	29/65
5	2.0[a]	27/16.4	33/55	23/55
6	2.0[b]	27.8/15.6	32/58	25/54
7	2.5	−/13.6	−/66	−/72
8	3.0	−/13.4	−/67	−/64
9	3.5	−/9.3	−/97	−/64
10	4.0	−/13.6	−/66	−/58

[a] The sample was prepared at 450 °C.
[b] The sample was prepared at 100 °C.
[c] As-prepared/calcined.

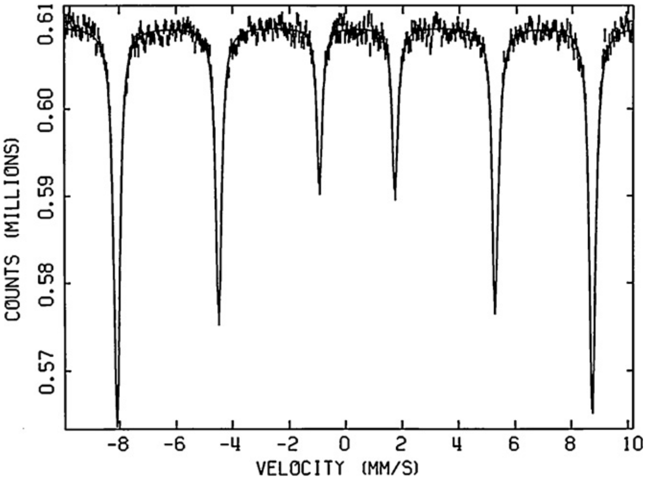

Fig. 3. Mossbauer spectrum of $LaFeO_3$ sample prepared at 100 °C.

cannot be compared in terms of crystallinity. Table 1 shows the particle sizes of perovskites calculated by Scherer equation. Particle size of the as-prepared and the calcined samples did not change much at lower GNR ($\leq$1.0). As the glycine concentration increased in the precursor solution, the particle size of the perovskites decreased until a GNR of 2.0 and remained constant with the further increase in GNR. It has been reported that the combustion temperature reach >1000 °C for samples prepared at a GNR of $\leq$1.0 [20]. This high temperature causes sintering of the particles, which explains the observed large particle size at lower GNRs. As the glycine concentration increases, the maximum attainable temperature decreases to <500 °C (GNR $\geq$ 2.0) [20]. This lower value of maximum attainable temperature in the combustion yields smaller $LaFeO_3$ particle size for samples synthesized at higher GNR. The amount of gaseous products generated also increases drastically above a GNR of 1.0. The large volume of the gas products at higher glycine concentration (GNR > 1.0) inhibits the sintering of the particles. Hence, smaller particle size can be noticed. $LaFeO_3$ samples prepared at 100 °C and 450 °C at a GNR of 2.0 were also found to be single-phase material. The particle size measurements carried out on these two samples are very close to that of the sample that was prepared at a GNR of 2.0 at 300 °C. It might be safely concluded from Figs. 1 and 2 that the temperature of preparation does not have any effect on the phase purity and the particle size of $LaFeO_3$.

3.2. BET surface area

Table 1 shows the BET specific surface areas of $LaFeO_3$ perovskite samples prepared at various GNRs and temperatures. The BET specific surface areas of $LaFeO_3$ samples, both as-prepared and calcined, increased with an increase in GNR up to 2.0 and remained nearly constant at higher GNRs. The increase

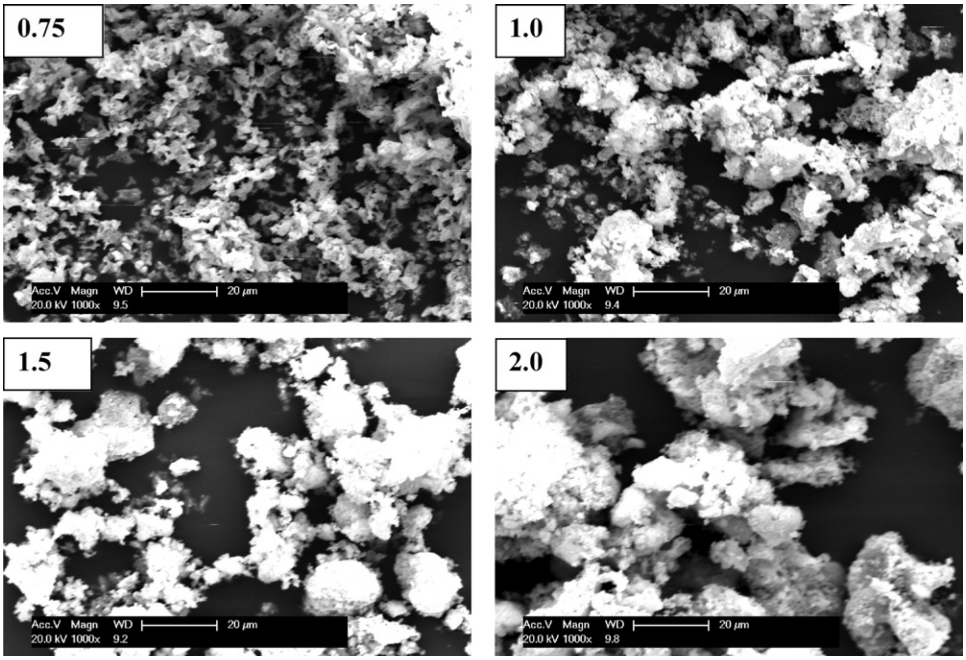

Fig. 4. Scanning electron micrographs of the as-prepared $LaFeO_3$ perovskites.

of surface areas is attributed to the higher amount of gaseous products produced at higher glycine concentration (GNR > 1.0). The gaseous products hinder the agglomeration of particles, which in turn inhibits the sintering of particles. The BET specific surface areas of the samples prepared above a GNR of 1.5 are higher than that of $LaFeO_3$ prepared by solid state reaction [15] and combustion [21].

The grain equivalent diameter (D_{BET}) has been calculated using BET specific surface area according to the following equation assuming that all the particles are spherical.

$$D_{BET} = \frac{6}{\rho S} \tag{1}$$

where, ρ is the theoretical density and S is the specific surface area of $LaFeO_3$. The particle sizes obtained from BET surface area and XRD are very similar, which indicates that there is minimal interparticle contact.

3.3. Mossbauer spectroscopy

The Mossbauer spectrum of $LaFeO_3$ sample prepared at a GNR of 2.0 is shown in Fig. 3. This sample was prepared at 100 °C. The Mossbauer spectrum showed narrow absorption lines of 0.25 mm/s. A least squares fit of the spectrum gave a value for the isomer shift $\delta = 0.36$ mm/s, for the quadrupole shift $2\varepsilon = -0.069$ mm/s and for the magnetic hyperfine field

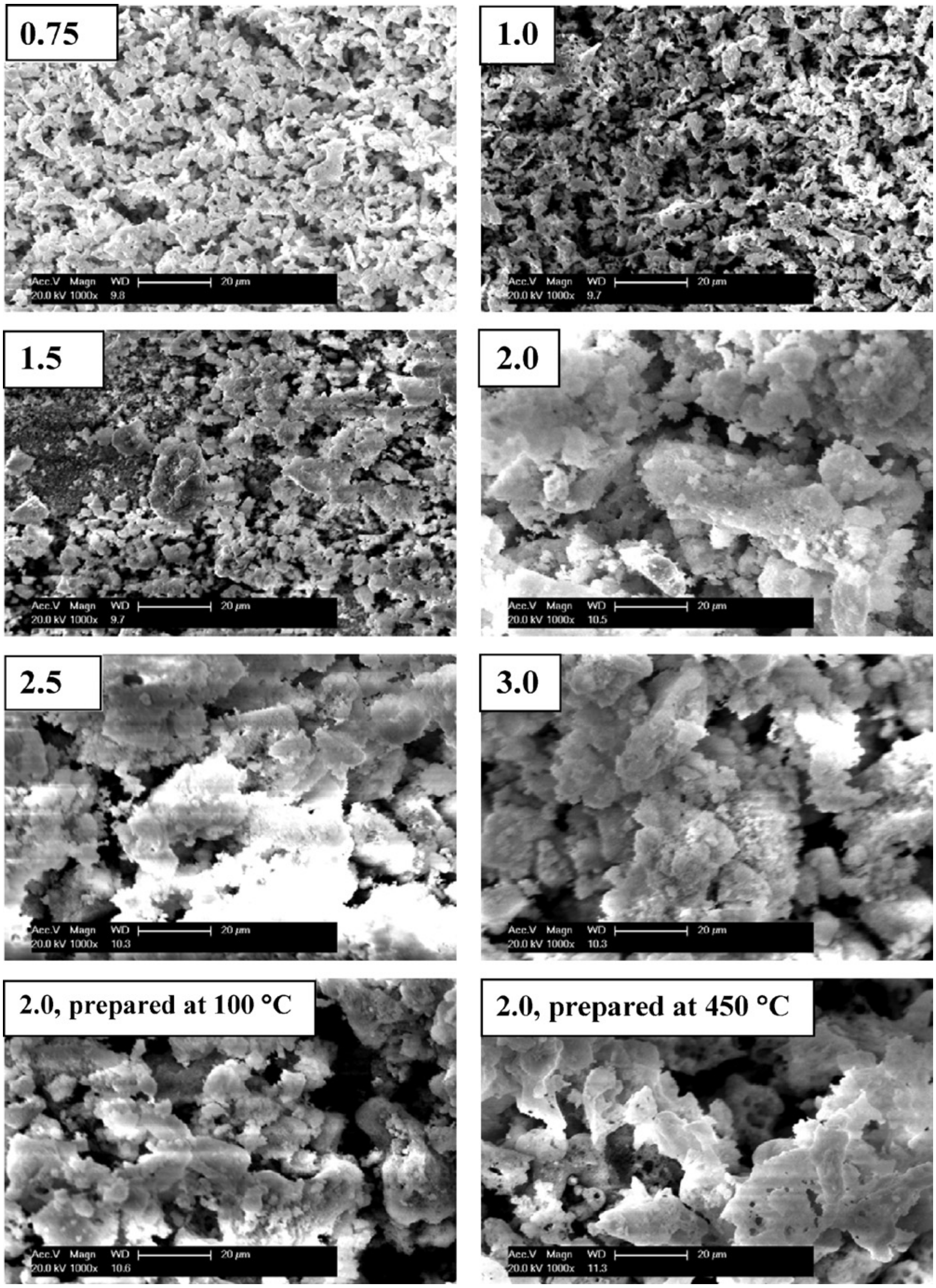

Fig. 5. Scanning electron micrographs of the calcined $LaFeO_3$ perovskites.

H_{hf} = 523.3 kOe. All these parameters confirm that the iron is in trivalent state [22]. A small concentration of Fe^{4+} was also present in the sample (<0.5%).

3.4. Scanning electron microscopy (SEM)

The SEM micrographs of the as-prepared $LaFeO_3$ samples are shown in Fig. 4. The grains are well separated in the sample prepared at a GNR of 0.75 but agglomeration can be noticed in the samples prepared at higher amounts of glycine. The samples prepared at higher GNRs (>0.75) also show the presence of porosity in the agglomerates. Fig. 5 shows SEM micrographs of the $LaFeO_3$ samples calcined at 700 °C. The samples prepared at lower amounts of glycine (GNR < 1.5) show the connected network of the particles. Partial agglomeration of the particles can be noticed in the sample prepared at a GNR of 1.5. The samples prepared at a GNR of 2.0 and above are completely agglomerated (Fig. 5). Although, the agglomerate size is larger, it can be noticed from Fig. 5 that the primary particle size is smaller than that of the samples prepared at lower amounts of glycine.

3.5. Transmission electron microscopy (TEM)

The TEM micrographs of two as-prepared $LaFeO_3$ samples are shown in Fig. 6. The particle size of the sample prepared at a GNR of 0.75 is higher (>100 nm) than that of the sample prepared at a GNR of 2.0 (<50 nm). The shape of the particles is irregular in both cases. The TEM particle sizes are in good agreement with the particle sizes estimated by XRD and BET data. Fig. 7 shows TEM micrographs of a few $LaFeO_3$ samples calcined at 700 °C for 2 h. The particles in the sample prepared at a GNR of 0.75 are agglomerated with a size of more than 100 nm, which is in good agreement with the particle size calculated by Scherer equation. As the amount of glycine increased in the precursors, the particle size decreased as can be observed from TEM micrographs. At lower glycine amounts, the synthesized particles are spherical, but as the glycine amount was increased the particles exhibited dumbbell-like shape. Jadhav et al. [23] observed rectangular polygon shape for $LaFeO_3$ samples prepared by co-precipitation method. The particle size in their work was 80 nm for the samples calcined at 450 °C. In the present study, smaller particle sizes were obtained (GNR $\geq$ 2.0) though the samples were calcined at much higher temperatures (700 °C).

3.6. Temperature-programmed reduction (TPR)

The TPR profiles of $LaFeO_3$ perovskites are shown in Fig. 8. No reduction of Fe was observed at low temperatures (<700 °C) for samples prepared at a GNR < 2.0. This observation is consistent with the other studies [3,24]. The samples prepared at a GNR of 2.0 and above showed peaks due to the reduction of Fe^{n+}. In another study, it was observed that $LaFeO_3$, prepared by the reactive grinding method, was reduced in two major steps, the first peak (~465 °C) was due to the reduction of Fe^{3+} to Fe^{2+} and the second peak (~750 °C) was due to the reduction of Fe^{2+} to Fe^0 [25]. The two shoulders at the beginning of the first peak were assigned to a small presence of Fe^{4+} and/or to a better reactivity of Fe^{3+} cations in the perovskite [25]. $LaFeO_3$ prepared by the citrate method also showed two reduction peaks [26,27].

It has been proposed that the reduction of Fe proceeds as follows [25]:

$$LaFe^{3+}O_3 + 1/2H_2 \rightarrow LaFe^{2+}O_{2.5} + 1/2H_2O \quad (2)$$

$$LaFe^{2+}O_{2.5} + H_2 \rightarrow 1/2La_2O_3 + Fe^0 + H_2O \quad (3)$$

The sample prepared at a GNR of 2.0 showed a peak at 370 °C. In the case of the sample prepared at a GNR of 3.0, a peak was observed at 386 °C. The peaks at 370 °C and 386 °C can be assigned to the reduction of Fe^{4+} as reported elsewhere [25]. These peaks were assigned to Fe^{4+} based on the literature data, but could also be due to Fe^{3+} as discussed in Mossbauer spectroscopy. The reduction profile of the sample prepared at a GNR of 3.5 showed a peak at 456 °C, which might be due to the reduction of Fe^{3+} [25]. The $LaFeO_3$ sample prepared at a GNP of 4.0 showed 3 peaks at 310 °C, 396 °C and 475 °C. The peaks observed at 310 °C and 396 °C

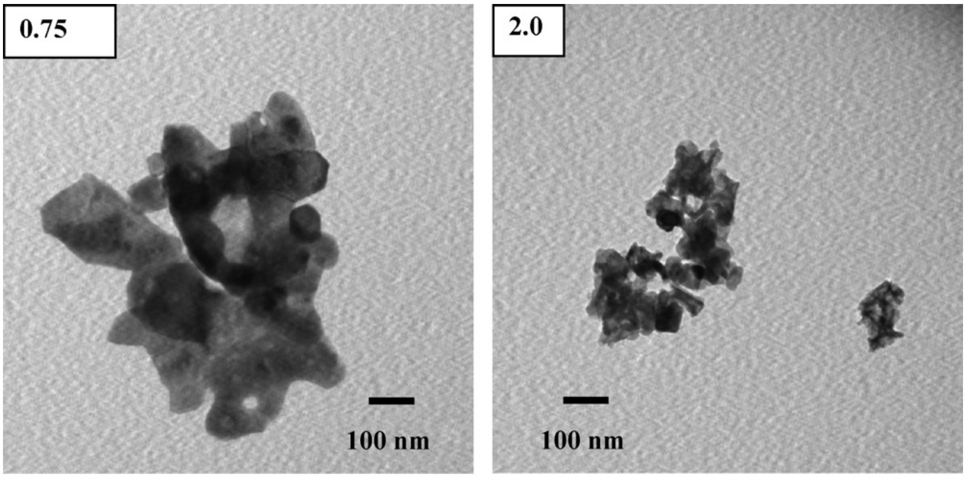

Fig. 6. Transmission electron micrographs of the as-prepared $LaFeO_3$ perovskites.

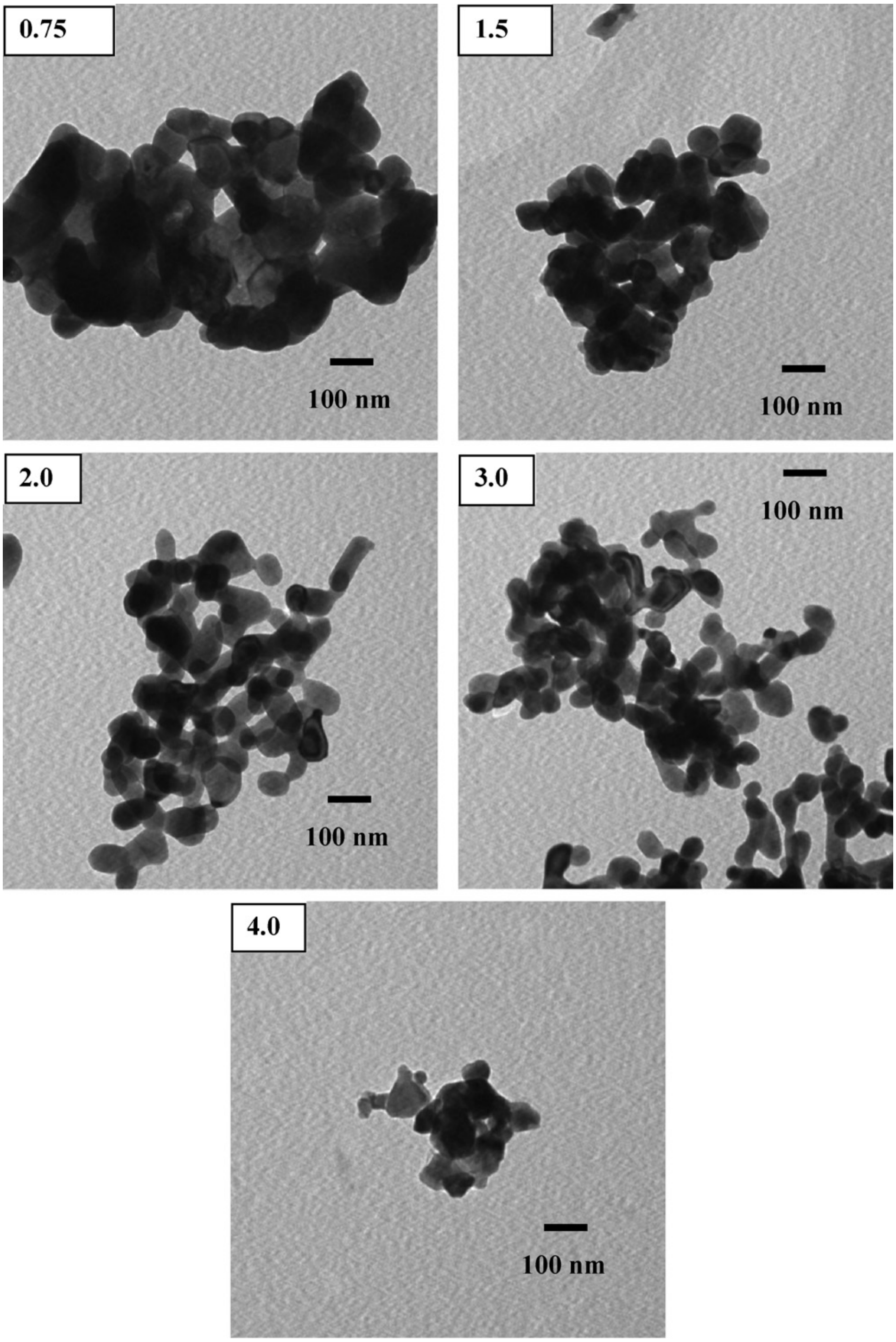

Fig. 7. Transmission electron micrographs of the calcined $LaFeO_3$ perovskites.

are likely due to the reduction of Fe^{4+} with different levels of interaction. The peak at 475 °C can be assigned to the reduction of Fe^{3+} [25]. All the samples showed a reduction response at temperatures nearly at or slightly above 700 °C due to the reduction of Fe^{n+} and the reduction did not complete even at the highest measurement temperature of 900 °C. The presence of the reduction peaks at higher amounts of glycine is attributed to the smaller particle size of $LaFeO_3$ and higher porosity.

In order to examine the effect of particle size/surface area on the reducibility of Fe^{n+}, $LaFeO_3$ sample (GNR = 4.0) was calcined at 700 °C for 12 h and 24 h to deliberately increase the particle size and to decrease the specific surface area. The BET specific surface areas of the two samples calcined for 12 h and 24 h are 7.0 and 4.3 m^2/g, respectively. The crystallite sizes (calculated using Scherer equation) of the two samples calcined for 12 h and 24 h are 100 and 130 nm, respectively (the XRD patterns are not shown here but were confirmed to be in

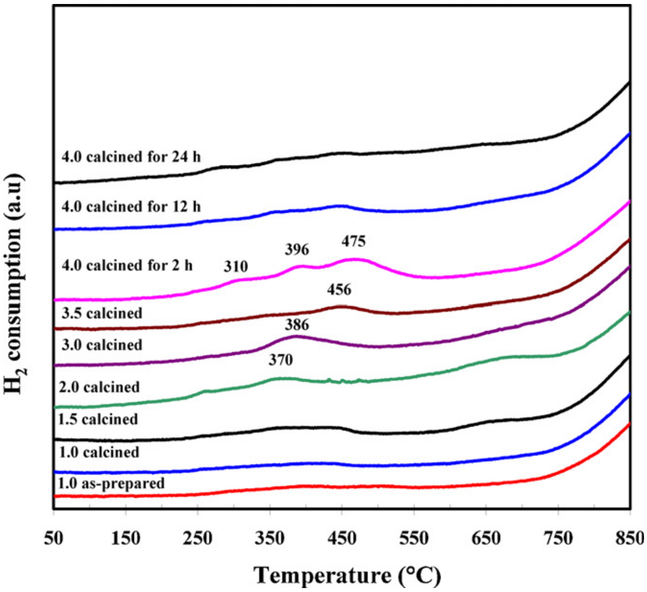

Fig. 8. Temperature-programmed reduction profiles of various perovskites.

orthorhombic phase). For same sample (GNR = 4.0) calcined at 700 °C for 2 h, the BET specific surface area and the particle size are 13.6 m^2/g and 58 nm, respectively. These results clearly show a significant coarsening effect of calcination for longer time. The TPR profiles of the two samples calcined for 2 and 12 h can be examined in the plots shown in Fig. 8. It can be noticed that the intensity of the peaks decreased drastically for 12 h calcined sample and also the peaks shifted to lower temperatures. The same phenomenon can be noticed for the sample calcined for 24 h. The decrease of peak intensities in TPR can be attributed either to the low porosity (low surface area), which reduces the diffusion of H_2 to the core of perovskite particles [26] or to the increase of particle size of $LaFeO_3$ as reported elsewhere for the ammonia synthesis catalysts [28]. Hence, the samples prepared at low GNRs (<2.0) did not show any reduction peaks or very low intense peaks due to the limited porosity or due to bigger particle size as discussed above (Table 1 and Fig. 7).

4. Conclusions

$LaFeO_3$ perovskite has been successfully prepared by the combustion technique with nanometer size and the effect of glycine concentration was studied on the properties of $LaFeO_3$. X-ray diffraction results showed the formation of orthorhombic perovskite phase irrespective of glycine concentration in the precursor and the temperature of preparation. The particle size of the synthesized perovskites decreased with an increase in a glycine-to-nitrate ratio (GNR) of up to 2.0 and was remained nearly constant with further increase in GNR. Correspondingly, the BET specific surface areas of the perovskites increased with an increase in a GNR of up to 2.0 and remained constant with the further increase in GNR. The surface area increased by two-fold for a GNR increase from 0.75 to 2.0. The particle size measurements by XRD, BET and TEM are in good agreement with each other. No reduction of Fe^{n+} was noticed at lower GNRs (≤1.5), but the reduction was observed >1.5 due to the increase of specific surface area and also due to the decrease of the particle size.

Acknowledgements

The authors are thankful to Bob Whitehead for the XRD analysis, Kathy Fulton for the BET analysis and Dr. Schurer for the Mossbauer analysis. The authors are also thankful to Ontario Fuel Cell Research and Innovation Network (OFCRIN) and NSERC for the financial support.

References

[1] K. Poplawski, J. Lichtenberger, F.J. Keil, K. Schnitzlein, M.D. Amiridis, Catalytic oxidation of 1,2-dichlorobenzene over ABO_3-type perovskites, Catal. Today 62 (2000) 329–336.
[2] G.S. Gallego, C. Batiot-Dupeyrat, J. Barrault, E. Florez, F. Mondragón, Dry reforming of methane over $LaNi_{1-y}B_yO_{3\pm\delta}$(B = Mg, Co) perovskites used as catalyst precursor, Appl. Catal. A: Gen. 334 (2008) 251–258.
[3] M.R. Goldwasser, M.E. Rivas, M.L. Lugo, E. Pietri, J. Pérez-Zurita, M.L. Cubeiro, A. Griboval-Constant, G. Leclercq, Combined methane reforming in presence of CO_2 and O_2 over $LaFe_{1-x}Co_xO_3$ mixed-oxide perovskites as catalysts precursors, Catal. Today 107–108 (2005) 106–113.
[4] J.P.P. Huijsmans, Ceramics in solid oxide fuel cells, Curr. Opin. Solid State Mater. Sci. 5 (2001) 317–323.
[5] S. Tao, J.T.S. Irvine, A redox-stable efficient anode for solid-oxide fuel cells, Nat. Mater. 2 (2003) 320–323.
[6] J.W. Fergus, Oxide anode materials for solid oxide fuel cells, Solid State Ionics 177 (2006) 1529–1541.
[7] A. Mai, V.A.C. Haanappel, S. Uhlenbruck, F. Tietz, D. Stöver, Ferrite-based perovskites as cathode materials for anode-supported solid oxide fuel cells: Part I. Variation of composition, Solid State Ionics 176 (2005) 1341–1350.
[8] C.B. Alcock, R.C. Doshi, Y. Shen, Perovskite electrodes for sensors, Solid State Ionics 51 (1992) 281–289.
[9] J. Topfer, J.B. Goodenough, Charge transport and magnetic properties in perovskites of the system La–Mn–O, Solid State Ionics 101–103 (1997) 1215–1220.
[10] A.B. Antunes, V. Gilc, C. Mourec, O. Pena, Magnetic properties of Er(Co, Mn)O_3 perovskites, J. Eur. Ceram. Soc. 27 (2007) 3927–3930.
[11] L. Bedel, A.C. Roger, C. Estournes, A. Kiennemann, Co^0 from partial reduction of La(Co, Fe)O_3 perovskites for Fischer–Tropsch synthesis, Catal. Today 85 (2003) 207–218.
[12] X. Dai, C. Yu, Q. Wu, Comparison of $LaFeO_3$, $La_{0.8}Sr_{0.2}FeO_3$, and $La_{0.8}Sr_{0.2}Fe_{0.9}Co_{0.1}O_3$ perovskite oxides as oxygen carrier for partial oxidation of methane, J. Nat. Gas Chem. 17 (2008) 415–418.
[13] D. Bayraktar, F. Clemens, S. Diethelm, T. Graule, J. Van herle, P. Holtappels, Production and properties of substituted $LaFeO_3$–perovskite tubular membranes for partial oxidation of methane to syngas, J. Eur. Ceram. Soc. 27 (2007) 2455–2461.
[14] J.R. Mawdsley, T.R. Krause, Rare earth-first-row transition metal perovskites as catalysts for the autothermal reforming of hydrocarbon fuels to generate hydrogen, Appl. Catal. A: Gen. 334 (2008) 311–320.
[15] Q. Zhang, F. Saito, Effect of Fe_2O_3 crystallite size on its mechanochemical reaction with La_2O_3 to form $LaFeO_3$, J. Mater. Sci. 36 (2001) 2287–2290.
[16] M. Kumar, S. Srikanth, B. Ravikumar, T.C. Alex, S.K. Das, Synthesis of pure and Sr-doped $LaGaO_3$, $LaFeO_3$ and $LaCoO_3$ and Sr, Mg-doped $LaGaO_3$ for ITSOFC application using different wet chemical routes, Mater. Chem. Phys. 113 (2009) 803–815.
[17] Z. Zhong, L. Chen, Q. Yan, X. Fu, J. Hong, Study on the preparation of nanometer perovskite-type complex oxide $LaFeO_3$ by sol–gel method, Stud. Surf. Sci. Catal. 91 (1995) 647–655.

[18] G. Shabbir, A.H. Qureshi, K. Saeed, Nano-crystalline $LaFeO_3$ powders synthesized by the citrate–gel method, Mater. Lett. 60 (2006) 3706–3709.

[19] X. Qi, J. Zhou, Z. Yue, Z. Gui, L. Li, Auto-combustion synthesis of nanocrystalline $LaFeO_3$, Mater. Chem. Phys. 78 (2002) 25–29.

[20] K. Deshpande, A. Mukasyan, A. Varma, Direct synthesis of iron oxide nanopowders by the combustion approach: reaction mechanism and properties, Chem. Mater. 16 (2004) 4896–4904.

[21] Y. Wang, J. Zhu, L. Zhang, X. Yang, L. Lu, X. Wang, Preparation and characterization of perovskite $LaFeO_3$ nanocrystals, Mater. Lett. 60 (2006) 1767–1770.

[22] N.A. Merino, B.P. Barbero, P. Ruiz, L.E. Cadus, Synthesis, characterisation, catalytic activity and structural stability of $LaCo_{1-y}Fe_yO_{3\pm\lambda}$ perovskite catalysts for combustion of ethanol and propane, J. Catal. 240 (2006) 245–257.

[23] A.D. Jadhav, A.B. Gaikwad, V. Samuel, V. Ravi, A low temperature route to prepare $LaFeO_3$ and $LaCoO_3$, Mater. Lett. 61 (2007) 2030–2032.

[24] G. Pecchi, P. Reyes, R. Zamora, C. Campos, L.E. Cadus, B.P. Barbero, Effect of the preparation method on the catalytic activity of $La_{1-x}Ca_xFeO_3$ perovskite-type oxides, Catal. Today 133–135 (2008) 420–427.

[25] B. Levasseur, S. Kaliaguine, Methanol oxidation on $LaBO_3$ (B = Co, Mn, Fe) perovskite-type catalysts prepared by reactive grinding, Appl. Catal. A: Gen. 343 (2008) 29–38.

[26] P. Ciambelli, S. Cimino, L. Lisi, M. Faticanti, G. Minelli, I. Pettiti, P. Porta, La, Ca and Fe oxide perovskites: preparation, characterization and catalytic properties for methane combustion, Appl. Catal. B: Environ. 33 (2001) 193–203.

[27] B.P. Barbero, J.A. Gamboa, L.E. Cadus, Synthesis and characterisation of $La_{1-x}Ca_xFeO_3$ perovskite-type oxide catalysts for total oxidation of volatile organic compounds, Appl. Catal. B: Environ. 65 (2006) 21–30.

[28] F. Pinna, T. Fantinel, G. Strukul, A. Benedetti, N. Pernicone, TPR and XRD study of ammonia synthesis catalysts, Appl. Catal. A: Gen. 149 (1997) 341–351.